RESEARCH ARTICLE OPEN ACCESS

Synthesis Characterization and Properties of Silica-Nickel Nanocomposites through Chemical Route

A.K.Pramanick
Metallurgical and Material Engineering Department Jadavpur University, Kolkata- 700032, India.

Abstract:
There has been an increasing demand for high performance Nanocomposites which can withstand several conditions such as low and high temperature, pressure and atmosphere in various applications. In order to meet these demands, SiO_2-Nickel Nanocomposites can be explored for important applications in various industries. Metals having sizes of the order of a few nanometers dispersed in silica matrix and their sintering mechanism have been discussed in this work. A Niihara approach is chosen to measure the micro-fracture toughness of silica-nickel Nanocomposites for both type of cracks found in this work.

Keywords: Nanocomposites, sintering, micro-fracture toughness, Palmqvist crack, Median crack, Nickel, Niihara

Nanocomposites consist of two or more phases, at least one phase having nanometer dimensions. A particular case is the dispersion of nanometer size phase within a host ceramic matrix. Ceramic materials are inherently resilient to oxidation and deterioration at elevated temperature. Some of these materials would be ideal candidates for use in high-temperature and severe stress applications, especially for components in automobile, aircraft, gas turbine engines and cutting tools. Fracture toughness values for ceramics materials are low and typically lie between 1 and 5 Mpa $m^{1/2}$. By way of contrast, Kc values for most metals are much higher and lie in the range 15-150 Mpa $m^{½}$ [1]. The fracture toughness of ceramics /Silica can also be improved significantly by the development of new generation of ceramic/silica based metal like Ni, Co, Cu, Fe etc Nanocomposites.
Synthesis and characterization of nanostructured materials have recently been studied world over and effort has been given for basic understanding [2-4]. In the last two decades synthesis, characterization and understanding a material with lower dimensions have become the most interesting area of research due to their novel properties and potential applications in different fields [5-9]. The transition metal nanoparticles such as Fe, Co and Ni have been given much attention due to their various applications in electronic, optical, and magnetic, recording , superconductors, mechanical devices and so on [10-14].

In this present work, Silica-Nickel Nanocomposites have been developed by chemical route followed by their characterizations to be established. Silica-Nickel Nanocomposites powders developed by chemical route were used as a starting material for the study of sintering mechanism. This work focused on the relationship between the densification parameters and material properties of Silica-Nickel Nanocomposites depending on the Nickel contents and sintering temperature. Micro indentation method which does not require any specific geometry for the test specimen was used to evaluate the fracture toughness in this work.

I. Experimental procedure

Silica – Nickel Nanocomposites was synthesized using commercial silica gel powder by chemical route. In this typical process, each one with 1.44gm powder silica powder in the size range (100-200 mesh) is mixed with a homogeneous solution with 1 ml of distilled water, containing required amount of $NiCl_2$, 100% excess glucose over stoichiometric requirement of complete reduction of $NiCl_2$ and stirred manually to prepare a homogeneous mixture . The resulting mixture is left for drying at room temperature. By this process, we also prepare the samples for 5 wt%, 10 wt%, 15 wt%, 20 wt% of Nickel with 100% excess glucose over that required for the complete reduction of $NiCl_2$. The chemical composition of the samples is summarized in Table-1.

Table 1: Chemical composition of samples

Samples	Water(H_2O) (cc)	Amt. of $NiCl_2$ (gm)	Amt. of Dextrose (gm)
Commercial grade silica-5wt% Nickel	1	0.16	0.07
Commercial grade silica-10wt% Nickel	1	0.32	0.14
Commercial grade silica-15wt% Nickel	1	0.48	0.22
Commercial grade silica-20wt% Nickel	1	0.64	0.29

Each dried sample containing Nickel chloride was reduced in tubular furnace at a temperature of 550^{o}C under the controlled flow of nitrogen for a period of 12 minutes. During heating, the dextrose breaks into carbon and water vapour which again react to produce in situ hydrogen. This in-situ generated H_2 in the nanopores reduces the $NiCl_2$ to metallic Nickel[15] as per the following reactions.

$C_6H_{12}O_6 \rightarrow 6C + 6H_2O.$ (1)
$6H_2O + 6C \rightarrow 6CO + 6H_2$ (2)
$NiCl_2 + H_2 \rightarrow Ni + 2HCl$ (3)

The obtained Nanocomposites have been characterized by X-ray diffraction (XRD), transmission electron microscopy (TEM). The phase composition of the powders was determined by XRD using Cu K_α monochromatic radiation in Regaku make ultima III, XRD instrument. The TEM images have been recorded with a JEOL JEM 1010 microscope. The sizes of nanoparticles from each TEM image were measured and the corresponding size histograms have been realized using specific software.
For the study of sintering mechanism, pellets of 15mm dia & 10mm height of ground Silica-Nickel Nanocomposites are ground thoroughly in a mortar pastle and then about 3 drops of water is added for per gram of Nanocomposites powder and mixed thoroughly, followed by uniaxial 5-ton load to yield a It is to be noted that friction is large among Silica-Nickel Nanocomposites powder during compaction. Thus, it is difficult to get dense green compaction. The use of water acts as a lubricant to yield comparatively dense green compact.
The pellets made from different samples as isothermally heated over the temperature range 1100^{o}C – 1250^{o}C for a fixed period of sintering time of 120 minutes in nitrogen atmosphere. After sintering the diameter of the pellets are measured. Densification is then calculated by the relative shrinkage given by

$$\text{Densification} = \Delta d/d_i = \frac{(d_i - d_f)}{d_i} \quad (4)$$

Where d_i & d_f stand for the diameter of the cylindrical sample before and after sintering.

Samples for the indentation toughness measurements were polished with fine alumina powder on the glass until mirror like surface is achieved. Vickers indentations were made at test loads of 300, 500, 1000, 2000, 5000gf and 10,000gf using a commercial hardness testing machine. The loading time was fixed at 10s. the indentation sizes and the crack lengths were measured immediately after unloading.
The Vickers micro-hardness were calculated by the following equation

$$Hv = 463.6\ P/a^2 \text{ (Gpa)} \quad (5)$$

The Elastic Modulus of the sample was measured using Dynamic Elastic Properties Analyzer(DEPA).
The identification of the type crack is essential to the evaluation of the fracture toughness by the indentation micro fracture techniques. The relationship of crack length(l) and Indentation load(p) for the four different silica-nickel Nanocomposites possesses a distinct knee of transition at critical test load.
Distinct linearity exists in the region where load P is less that of the knee. In the regions higher than the critical load, linearity of data is not as good. Therefore, below this load, crack region is palmqvist and above is median crack region. Using equation of Nihara et al [eq6] and Nihara et al [eq. 7] fracture toughness for above samples were evaluated both for palmqvist and median type of crack respectively.

Palmqvist Cracks
Niihara et al [15]

$$K_{IC}\,(\varphi/H\,a^{½})\,(H/E\,\varphi)^{0.4} = 0.035(l/a)^{-1/2} \quad (6)$$

Median cracks
Niihara et.al [15],

$$K_{IC}\,(\varphi / Ha\ ½)\,(H / E\,\varphi)^{0.4} = 0.129\,(c/a)^{-3/2} \quad (7)$$

In the above equation φ is the ratio of the hardness to the yield stress, ($H_v/\sigma y$), which is about 3.

Results and discussion

Fig.1& Fig.2 represent the typical XRD patterns of commercial silica gel samples containing 5 wt% & 20 wt% Nickel, respectively. The highest intensity peak in each case has been used to compute the size of the Nickel using Scherrer formula[16] and tabulated in Table2.
The Table.2 contains the particle sizes of Nickel for different samples and it is found that 36 nm, 42 nm, 51 nm and 61 nm for commercial silica-5 wt%, 10 wt% 15, wt%, and 20 wt% Nickel Nanocomposites respectively.
The d_{hkl} value of each is computed and compared with the standard d_{hkl} values of metallic Nickel. This comparison is shown in Table 3. From the table we observe that the comparison is good. This suggests the preparation of pure metallic Nickel. In each figure, peaks corresponding to Nickel are marked, The value of $Sin\theta/\lambda$ in each of samples for the hump is 0.117, very close to 0.12 which is attributed to amorphous silica[17]. This is plausibly due to slow kinetics of crystallization of amorphous silica arising out of lower reduction temperature for a shorter period of time.
Fig.3 & Fig4 represent the typical TEM image of the commercial silica - 5 wt% Nickel & 20wt% Nickel Nanocomposites. Fig.3& Fig.4 showing the nickel particles of nanometric dimension are clearly visible in TEM images.
Fig.5 & Fig. 6 represent the typical SAED (Selected Area Electron Diffraction) pattern for the commercial silica - 5 wt% Nickel & 20wt% Nickel Nanocomposites. SAED pattern of the samples were used to compute the interplanar spacing and compare with the standard d_{hkl} of Nickel. Table 3 shows that the agreement between the standard and experimental d_{hkl} are good. This suggest that d_{hkl} of Ni and this is agree mental with the findings of XRD (Ref. JCPDS)
Fig.7 Fig 8 represent the lattice image, from which the interplanar spacing were measured directly which coincide with the standard value of metallic nickel.

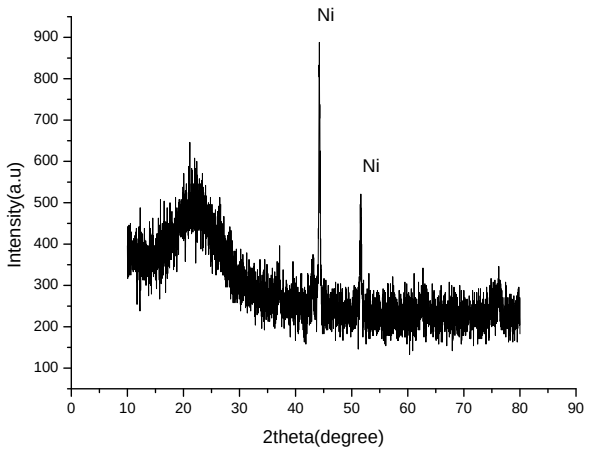

Fig. 1 XRD pattern of sample containing commercial grade Silica - 5wt% Nickel heat treated at 550^{o}C for 12 minutes in nitrogen atmosphere

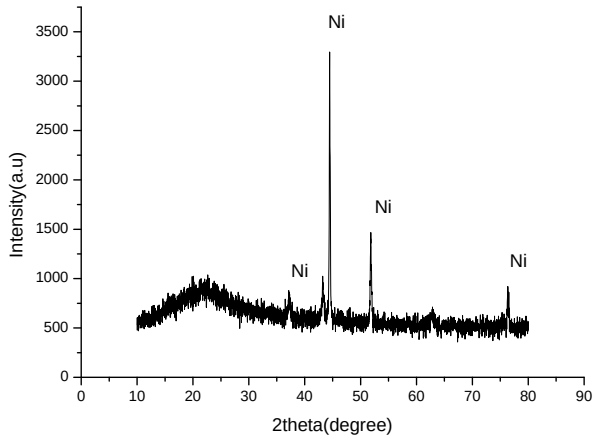

Fig. 2 XRD pattern of sample containing commercial grade Silica - 20wt% Nickel heat treated at 550^{o}C for 12 minutes in nitrogen atmosphere

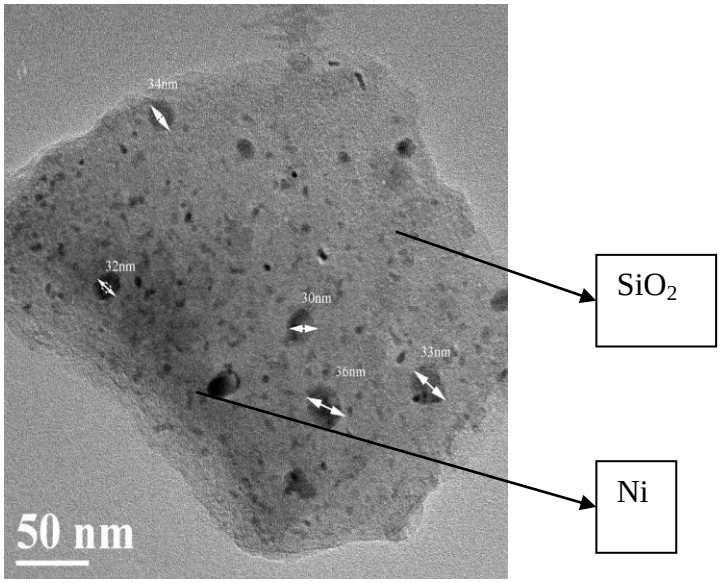

Fig. 3 TEM image of sample containing commercial grade Silica - 5 wt% Nickel

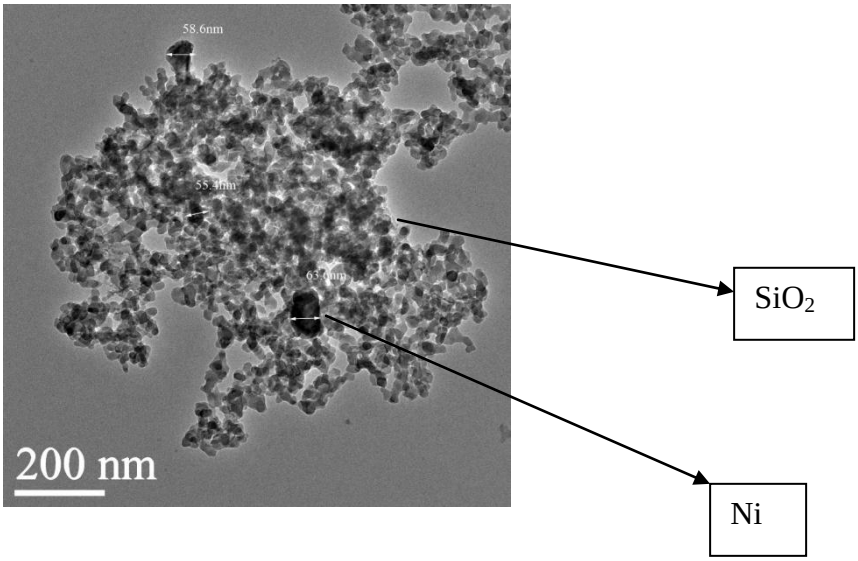

Fig. 4 TEM image of sample containing commercial grade Silica - 20 wt% Nickel

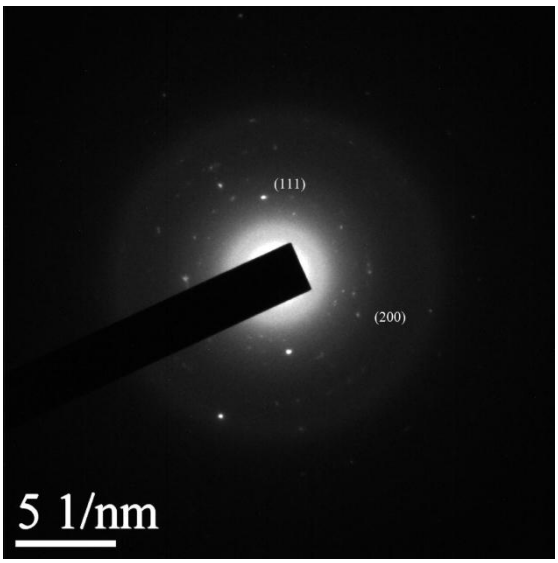

Fig. 5 SAED pattern of sample containing commercial grade Silica -5 wt% Nickel

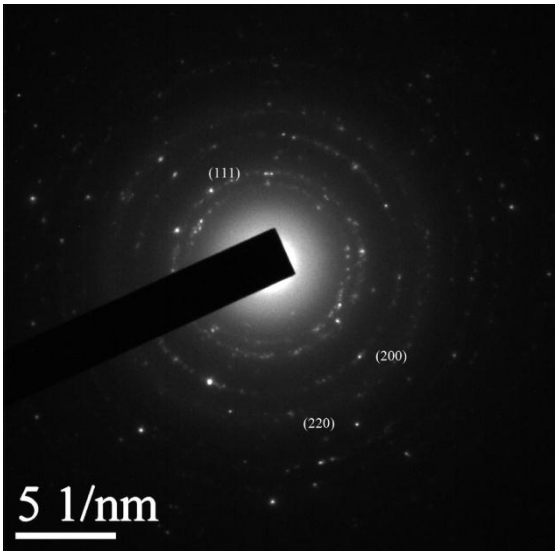

Fig. 6 SAED pattern of sample containing commercial grade Silica -20 wt% Nickel

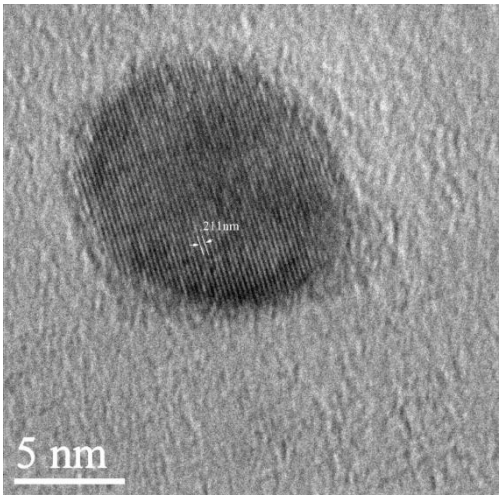

Fig.7 Lattice image of sample containing commercial grade Silica -5 wt% Nickel

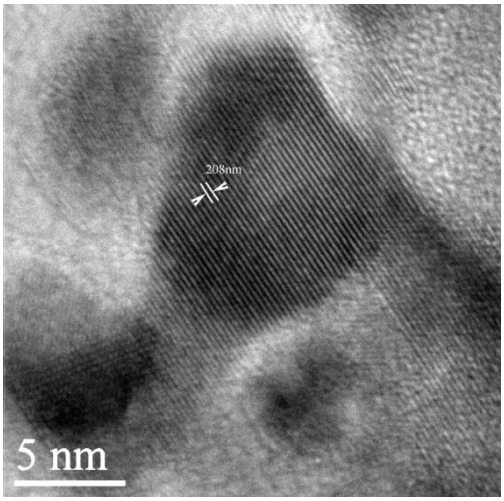

Fig. 8 Lattice image of sample containing commercial grade Silica -20 wt% Nickel

Table 2 contains the particle sizes of Nickel

Samples	Nickel crystallite size from XRD	Nickel particle size from TEM image
Commercial grade Silica-5wt% Nickel	36nm	38nm
Commercial grade Silica -10wt% Nickel	42nm	45nm
Commercial grade Silica -15wt% Nickel	51nm	54nm
Commercial grade Silica -20wt% Nickel	61nm	63nm

Table 3 contains interplanar spacing and compare with the standard d_{hkl} of Nickel

Samples	$d_{(111)}$ value from XRD	d value from TEM lattice image	$d_{(111)}$ value from SAED pattern	$d_{(111)}$ value from JCPDS Card No. 03-1051
Commercial grade Silica -5wt% Nickel	0.204 nm	0.211 nm	0.206 nm	0.202 nm
Commercial grade Silica -10wt% Nickel	0.203 nm	0.210 nm	0.212 nm	0.202 nm
Commercial grade Silica -15wt% Nickel	0.203 nm	0.208 nm	0.206 nm	0.202 nm
Commercial grade Silica -20wt% Nickel	0.203 nm	0.209 nm	0.209 nm	0.202 nm

The densification as a function of nickel content at 1250 ^{o}C for 120 minutes is summarized in the table 4. Table 4 and corresponding Fig 9 shows variation of densification as function of nickel content during isothermally sintered at 1250^{o}C for a fixed period of time. The kinetic of sintering is influenced by the temperature and duration of time employed. The Fig exhibits that for any fixed content of nickel, initially the rate is slow followed by slow rate of densification due to start with prior to formation of liquid, the system is more porous. Thus, the formation of liquid with time increases which causes rearrangement of powder packing by surface tension immediately and increases densification with increased amount of nickel content.

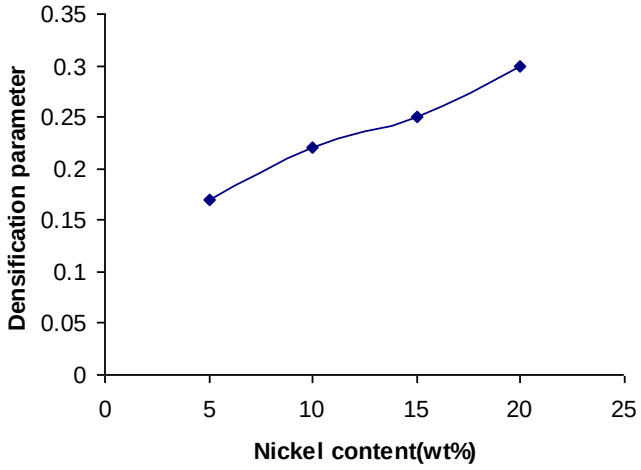

Fig. 9 Relationship between Densification parameter and Nickel content.

Table 4 Densification parameter vs Nickel content

Samples	Densification Parameter, Δd/d
Commercial grade Silica -5wt% Nickel	0.17
Commercial grade Silica -10wt% Nickel	0.22
Commercial grade Silica -15wt% Nickel	0.25
Commercial grade Silica -20wt% Nickel	0.30

The Vickers Micro-hardness(Hv) and Elastic modulus (E) of the samples were measured in the Table 5. Table 5 shows the comparison of micro hardness and elastic modulus as function of nickel content. From the Table 5 and also Fig.10 and Fig.11 it is observed that both micro-hardness and elastic modulus values are increasing with nickel content.

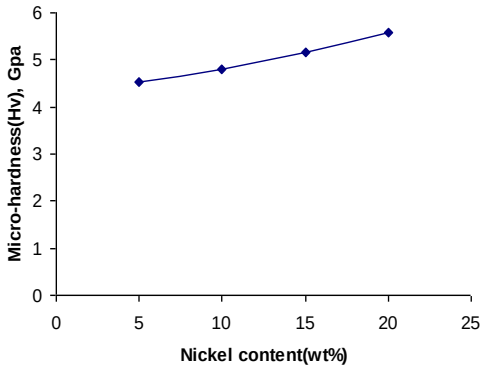

Fig. 10 Micro- hardness as function of Nickel content(wt%)

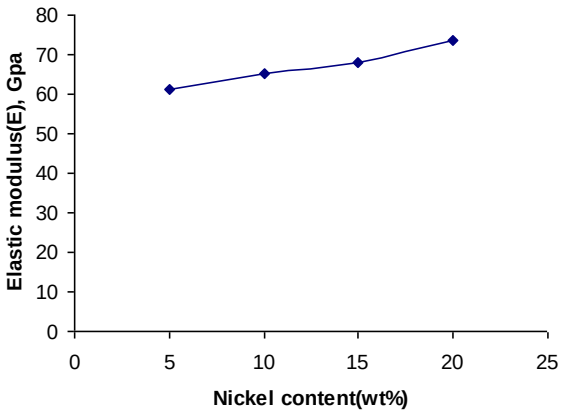

Fig. 11 Elastic modulus as function of Nickel content

Table 5 Comparison of micro- hardness and elastic modulus vs Nickel content(wt%)

Samples	Micro-hardness(H_v) Gpa	Elastic Modulus(E) Gpa
Commercial grade Silica -5wt% Nickel	4.52	61.15
Commercial grade Silica -10wt% Nickel	4.80	65.20
Commercial grade Silica -15wt% Nickel	5.16	68.11
Commercial grade Silica -20wt% Nickel	5.57	73.60

Fracture toughness vs. different loads for both types of cracks for all compositions of samples and the corresponding data are included in table 6 and table 7 and are depicted as the function of test load P in Fig.12 & Fig.13 respectively. These results exhibit a range of values from 1.81-3.71 Mpa m $^{-1/2}$. The results indicate that fracture toughness of Silica-Nickel Nanocomposites increases with nickel content. With increase in load, the fracture toughness changes hardly (change is in two order of magnitude) whereas the increase in nickel content there is significant change in fracture toughness This is amply clear from the visual inspection of Fig. 12 and Fig. 13 This is attributed due to the fact that with more of nickel content, the probability of crack being arrested during propagation is more and this makes the fracture toughness of the sample more.
Similar observation was found for median type of crack at high load. Only change of fracture toughness with load is more when compared with palmqvist type of crack. Fig15 & Fig 16 represent the typical micro crack indentation of Silica-5wt% and 20 wt% Nickel samples respectively.

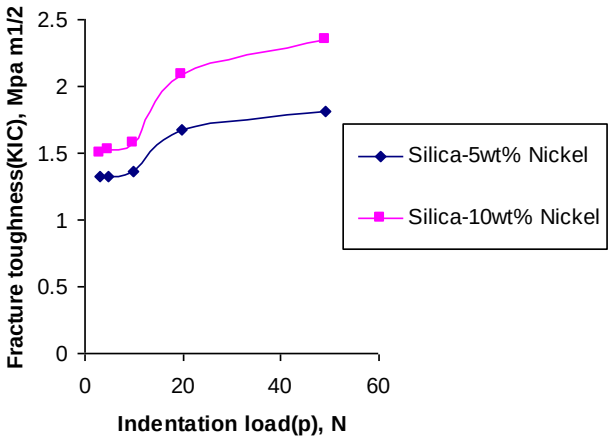

Fig. 12 Fracture toughness(Mpa m ^{½}) according to Palmqvist crack model and Median crack model as function of indentation load.

Table. 6 Indentation load(p) vs Fracture toughness(Mpa m ^{½})

Indentation load(p),N	Fracture toughness(Mpa m ^{½})	
	Commercial grade Silica-5wt%Nickel	Commercial grade Silica-10wt%Nickel
2.94	1.32	1.50
4.90	1.33	1.52
9.81	1.36	1.57
19.62	1.67	2.09
49.05	1.81	2.35

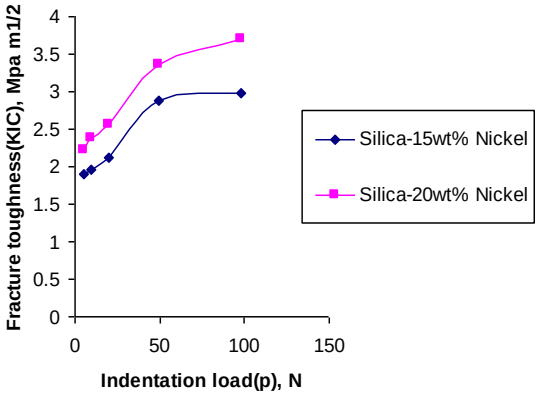

Fig. 13 Fracture toughness(Mpa m ^{½}) according to Palmqvist crack model and Median crack model as function of indentation load.

Table. 7 Indentation load(p) vs Fracture toughness(Mpa m ^{½})

Indentation load(p),N	Fracture toughness(Mpa m ^{½})	
	Commercial grade Silica-15wt% Nickel	Commercial grade Silica-20wt% Ni
4.90	1.91	2.23
9.81	1.97	2.38
19.62	2.12	2.56
49.05	2.89	3.36
98.10	2.99	3.71

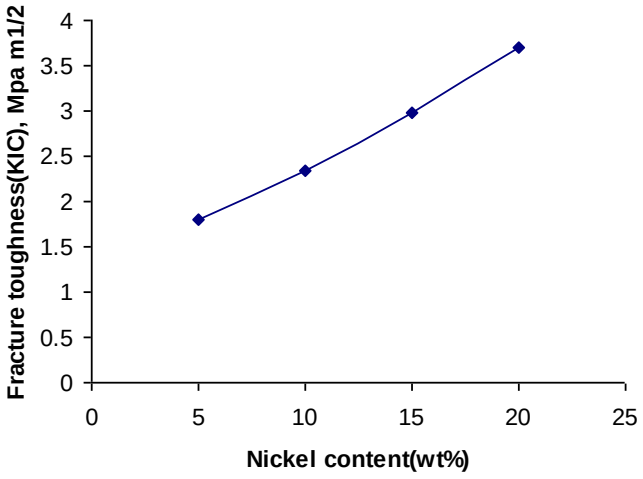

Fig. 14 Fracture toughness as function of Nickel content

Table 8 Comparison of Fracture toughness(Mpa m $^{1/2}$) vs Nickel content(wt%)

samples	Fracture toughness (Mpa m $^{1/2}$)
Commercial grade Silica-5wt% Nickel Nanocomposites	1.81
Commercial grade Silica-10wt% Nickel Nanocomposites	2.35
Commercial grade Silica-15wt% Nickel Nanocomposites	2.99
Commercial grade Silica-20wt% Nickel Nanocomposites	3.71

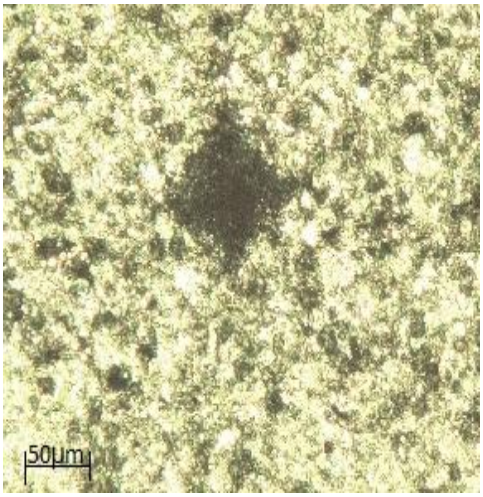

Fig. 15 Micro-crack indentation of sintered commercial grade Silica-5 wt% Nickel Nanocomposite

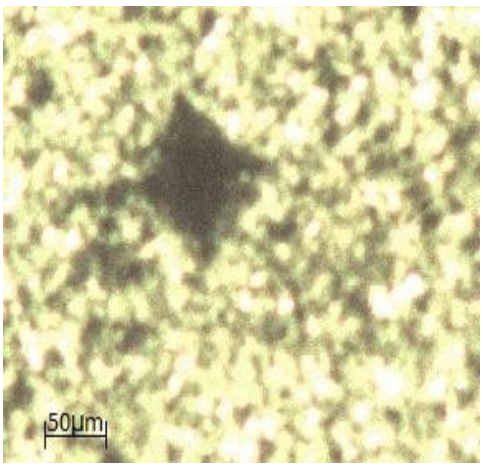

Fig. 16 Micro-crack indentation of sintered commercial grade Silica-20wt%Nickel Nanocomposite

Conclusions

1. Silica-Nickel Nanocomposites (using commercial grade silica) have been successfully synthesized via chemical route through in-situ reduction at 550^{o}C for different percentage of Nickel phase pure metallic has been confirmed by XRD & SAED analysis.
2. The particle size of Nickel computed by Scherrer formula is in the nanometric level as observed from the X-ray diffraction patterns. It is observed that the Nickel particle size ranging from 36 to 61nm for different Nickel content in the silica matrix from 5wt% to 20wt%, is in good agreement with obtained from TEM analysis.
3. Study of sintering behaviour of commercial grade Silica-Nickel powder shows that the densification parameter increases with temperature and maximum densification can be obtained at 1250^{o}C for 2 hours and also shows that sintering temperature is the main factor which determines densification.
4. Micro-hardness calculated from indentations is almost constant regardless of the test load.

5. The Micro hardness of Silica-Nickel Nanocomposites increases as the Nickel content in silica matrix increases and maximum value is achieved in Silica – 20 wt% Nickel Nanocomposites.
6. Fracture toughness of Silica-Nickel Nanocomposites for different compositions enhances significantly as Nickel content in the silica matrix increases and maximum value is achieved in Silica-20 wt% Nickel Nanocomposites.

References

[1.] Hull. D. T. W. Clyne. An Introduction to Composite Materials, 2nd edition, Cambridge Universitypress, New York, 1996.
[2.] Gao Y.Q, Bando Y, Nature, 415, 599, 2002.
[3.] Gorla C.R,Emanetoglu N.W, Liang S, Mago W.E, Lu Y, Wraback M, M..Shen M, Journal of Applied Physics. 85, 2595, 1999.
[4.] Aldal J, Rico- Gracia J.M, Lopez-Alonso J.M, Boreman S Nanotechnology 16, 230, 2005.
[5.] Gao Y.Q, Bando Y, Nature, 415 p. 599, 2002.
[6.] Rodriguez J. A, Jirsak T, J. Drorak, S.Sambasivan, D. Fischer, J. Phys. Chem.B 104,319, 2000.
[7.] Corla C.R, Emanetoglu N.W. Liang S.,.Mago W.E,.Wraback. Y.Lu, M, Shen H.J.Appl. Phys. 85, 2595, 1999.
[8.] Aldal J., Rico-Garcia J, M.Lopez- Alonso J.M, Boreman G, Nanotechlogy, 16 230, 2005.
[9.] .Lee J.H, Song W.C, Yi J.S., Yang K.J, Hang W.D, Thin Solid Films, 349, 431, 2003.
[10.] Prinz G.A., Science, 282,1660, 1998.
[11.] Khizroev S, Litvinov D, Nanotechnology, 15, 7, 2004.
[12.] Klimenkov M, Von Borany J, Matz W, Eckert D.,.Wolf M, Mueller K.H., Appl.Phys A 74 571, 2002.
[13.] Wagner M.L, Schmidt L.D, J.Phys.Chem,. 99, 805, 1995.
[14.] .Schmid G, Chi L.F, Adv. Mater,10, 515, 1998.
[15.] Das G.C, Basumallick A, Mukherjee S, 1990 Bulletin of Material Science, 13,255-258.
[16.] Cullity B.D, 1978 Elements of X-ray Diffraction, Addison-Wesley, Reading, Mass.
[17.] Warren B.E and.Biscal J, Am 1938 J. Ceram. Soc,21, 49